

Article

A Four-Winding Inductive Filtering Transformer to Enhance Power Quality in a High-Voltage Distribution Network Supplying Nonlinear Loads

Yuehui Chen ¹, Zhao Huang ², Zhenfeng Duan ¹, Pengwu Fu ¹, Guandong Zhou ¹ and Longfu Luo ^{2,*}

¹ State Grid Hunan Electric Power Company, Changsha 410012, China; Chenyh6@hn.sgcc.com.cn (Y.C.); duanzf@hn.sgcc.com.cn (Z.D.); fupw@hn.sgcc.com.cn (P.F.); zhougd@hn.sgcc.com.cn (G.Z.)

² The College of Electrical and Information Engineering, Hunan University, Changsha 410082, China; huangpowers@163.com

* Correspondence: llf@hnu.edu.cn

Received: 26 April 2019; Accepted: 24 May 2019; Published: 27 May 2019



Abstract: This paper solves the problem of reactive power and harmonics compensation in a high-voltage (HV) distribution network supplying nonlinear loads. An inductive filtering (IF) approach where passive filters connect to the filtering winding of a four-winding inductive filtering transformer (FW-IFT) is presented to enhance the power quality of the public grid. This method can not only greatly suppress harmonic currents of the medium and/or low-voltage (LV) side, but also prevent them from flowing into the public grid. The new main circuit topology, where the FW-IFT has specific filtering winding by adopting the ampere-turn balance of the transformer, is presented. On the basis of the structure of the FW-IFT, the magnetic potential balanced equation and inductive filtering technology, its equivalent circuit and mathematical model are established, and the filtering performances are analyzed in detail. Simulation and experimental results rated at SN-10/0.38 of the FW-IFT are presented to prove the efficacy of the comprehensive enhancement of power quality on the grid side.

Keywords: Four-winding inductive filtering transformer (FW-IFT); inductive filtering (IF); power quality; nonlinear loads; passive filter

1. Introduction

In recent years, a significant amount of nonlinear industrial and commercial loads, such as power electronic equipment, arc furnaces and electrical drives, are being applied in the high-voltage (HV) distribution network. These nonlinear characteristic harmonics generated by nonlinear loads will freely enter into the utility grid through transformers. Thus, it inevitably brings power-quality (PQ) problems to the HV distribution network [1–6]. Therefore, it is necessary to perform harmonic suppression and enhance the grid supply quality by means of a new device and applicable approach. In order to reduce the flow of harmonic currents from the load side to the utility grid, harmonic mitigation techniques are very important to improve the quality of grids in a HV distribution network. The traditional passive filter comprised of a capacitor and an inductor widely contributes to improve the power quality of the HV distribution network [7–10]. These filters have the advantage of being the preferred harmonic filtering solution, mainly for their high efficiency, low-cost, and simplicity. However, these characteristics of passive filters may deteriorate because of their dependence on the source impedance, in addition to the possibility of the occurrence of series and/or parallel resonance, which may lead to excessive harmonic amplification [11–13]. Thus, the filtering capability of passive filters is maintained by extra calibrating work.

A variety of active filtering approaches have been proposed to address these harmonic problems. Active filters applied for compensating harmonic currents of nonlinear loads provide good harmonic suppression, and they are suitable for small-rating nonlinear loads. However, a key issue for active filters is to find a control approach, which quickly obtains the compensation reference current without errors [14]. Hybrid active filters utilize the current modulation technique, and are characterized by a combination of passive filters and active filters. They were presented to eliminate current harmonics, and so they are cost effective and practical for large-rated nonlinear loads. However, this method needs tuned passive filters or extra matching power transformers to guarantee filtering performance [15–19].

In this paper, we provide an effective solution to reduce the harmonic distortion and increase the power quality of the utility grid. Firstly, a novel inductive filtering (IF) method with a four-winding inductive filtering transformer (FW-IFT) is put forward to apply in a HV distribution network, which can effectively enhance the power quality of the utility grid. Then, the mathematical modeling and the theoretical analysis are carried out in detail. Finally, both the simulation results and the prototype experiment are used to validate the good performance of the HV distribution network on harmonic suppression and reactive power compensation.

Since the IF method is different between active and passive filtering methods, it is the preeminent solution against nonlinear loads, which it achieves by fully utilizing the electromagnetic inductive filtering principle of the transformer, which is applied in the industrial direct-current (dc) supply system and high voltage dc system [20–22]. For the four-winding inductively filtered rectifier transformer (FW-IFRT), the ratings of the wye-connected bank of secondary winding of the load side and the delta-connected bank of tertiary winding of the load side are selected to be same, permitting the cancellation of 5th and 7th order characteristic harmonics, while only containing 11th and 13th order characteristic harmonics at the grid side [21]. However, for the FW-IFT, the 5th, 7th, 11th, and 13th order characteristic harmonics still exist in the grid side because of the voltage level and load rating capacity of the medium voltage (MV) and low voltage (LV) sides. So, the FW-IFT is obviously different from the FW-IFRT in meeting inductive filtering constraints. On the basis of the equivalent zero impedance principle, the filtering winding within the FW-IFT is designed by adjusting the winding structure of the four-winding transformer. Meanwhile, the point of passive filters connected in series with the filtering winding within the FW-IFT is to act as the inductive filtering system. Moreover, it can generate reverse harmonic currents through the harmonic ampere-turns balance of the FW-IFT's internal coupling windings to compensate for harmonic currents from nonlinear loads. So, it can eliminate load harmonics and enhance the power quality of the utility grid.

The rest of the paper is organized as follows. The new main circuit topology is described in Section 2. The theoretical analysis of the FW-IFT is subdivided into the mathematical model, harmonic current equations and inductive filtering system compensation in Section 3. Section 4 presents the simulation and experimental study. Section 5 elaborates the conclusion.

2. New Main Circuit Topology

Figure 1 shows main circuit topologies for a HV distribution network, where unit No.1 is the passive filtering (PF) scheme, and unit No.2 is the IF scheme. These passive filters tuned at the 5th, 7th, 11th, and 13th harmonic frequencies are allocated in the LV bus of 35 kV of the three-winding transformer, as in the PF scheme. Therefore, the PF can eliminate the main characteristic harmonics produced by nonlinear loads at the LV side, whereas it cannot reduce them at the MV side, and thus it cannot meet the requirements of grid harmonic distortion. Hence, a novel IF method is proposed to enhance the power quality of the utility grid.

Different from unit No.1, unit No.2 describes the new main-circuit topology of the proposed IF method. In this unit, the FW-IFT has four windings, i.e., the primary (HV), the secondary (MV), the tertiary (LV), and the filtering winding. The passive filters, which consist of the fully tuned branches, are connected to the filtering winding to interface with the HV distribution network. More importantly, the filtering winding within the FW-IFT is designed by a special arrangement of transformer winding.

Compared with the PF method, the IF method can suppress current harmonics at the MV and/or LV sides. Thus, there are fewer harmonic components in the primary winding of the FW-IFT or the public grid. In this way, the harmonics of nonlinear loads cannot flow into the primary winding, the reactive power can be compensated for by neighboring the nonlinear loads, and the power factor can also be increased, so the effects of the harmonics and the reactive power on the FW-IFT can be decreased effectively. Moreover, the IF method is interfaced with the HV distribution network via the system impedance and the short-circuit impedance of the FW-IFT, so it has a significant ability to prevent harmonic resonance. Hence, it can provide an effective way to solve the power quality problems of the HV distribution network supplying nonlinear loads.

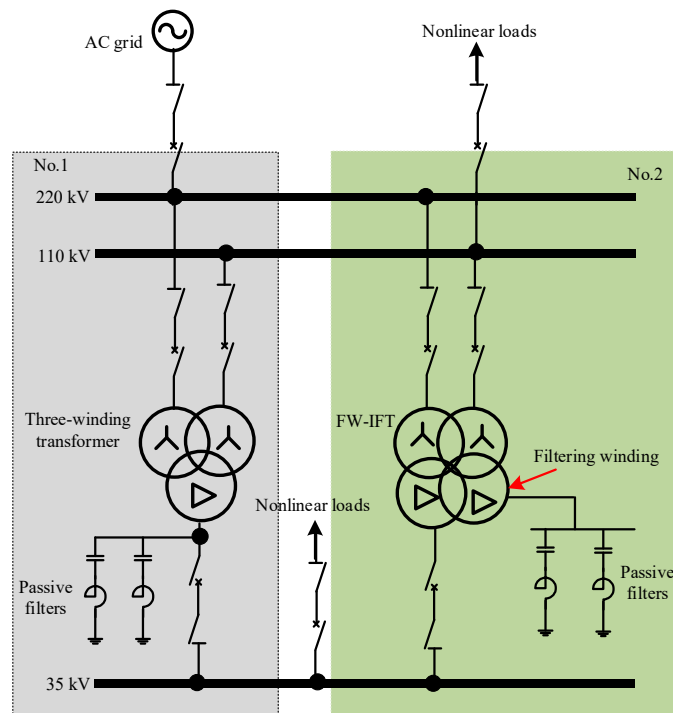


Figure 1. Main circuit topology for a high voltage (HV) distribution network with one passive filtering (unit No.1) and another inductive filtering (unit No.2). AC: alternative current; FW-IFT: four-winding inductive filtering transformer.

This HV distribution network mainly consists of the FW-IFT, passive filters, transmission line and loads. Figure 2 shows the wiring scheme of the FW-IFT. The core configuration of FW-IFT adopts the three-phase three limb. There are four windings on each iron beam, i.e., the wye-connected primary winding linked to the utility grid via the system impedance, the wye-connected secondary winding linked to the power load via the transmission line, the delta-connected tertiary winding linked to the power load via the transmission line, and the delta-connected filtering winding linked to the passive filters.

Regarding the FW-IFT, there are HV-, filtering-, MV-, and LV-winding, which is established in ANSOFT/MAXWELL software (ANSYS 16, ANSYS Inc, Shanghai, China), as shown in Figure 3.

Moreover, for the purpose of realizing the IF method, the FW-IFT needs a special winding-impedance design to coordinate the impedance of the fully tuned passive filters. In this way, the magnetic potentials of the 5th, 7th, 11th, and 13th harmonic currents produced by the nonlinear loads can be eliminated, which will be discussed in Section 3.

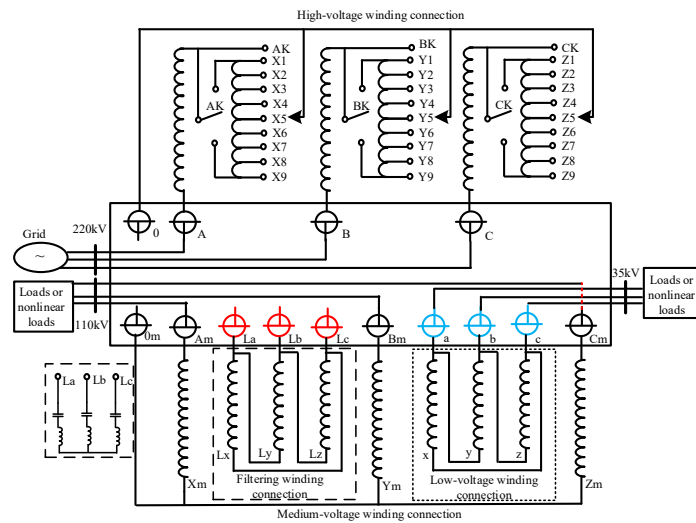


Figure 2. Wiring scheme of the FW-IFT and passive filters.

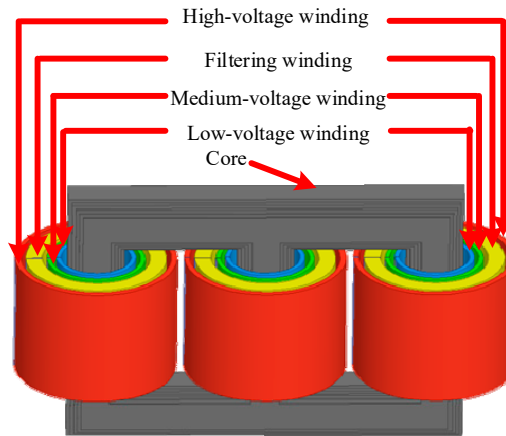


Figure 3. Three-dimensional finite element model of the FW-IFT.

3. Theoretical Analysis

3.1. Mathematical Model

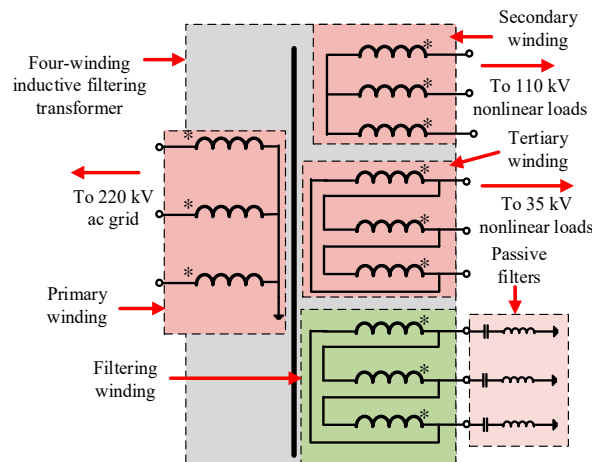
Figure 4 gives the three-phase structure and single-phase equivalent decoupling circuit of the FW-IFT. The three-phase construction of the FW-IFT, which consists of the primary, filtering, secondary, and tertiary winding connected to 220 kV alternative current (ac) grid with passive filters of 35 kV, 110 kV, and 35 kV nonlinear loads, respectively, is described in Figure 4a. As long as the equivalent impedances $Z_{K4,12}$ and $Z_{K4,13}$ are approximately equal to zero, the FW-IFT will satisfy the IF condition [21]. So the single-phase equivalent circuit model of the FW-IFT is a radial circuit, where includes the short-circuit impedance Z_{K14} , and equivalent impedances $Z_{K4,23}$, $Z_{K2,34}$, $Z_{K3,24}$, as shown in Figure 4b. At the same time, Figure 4c gives the simplified resistive equivalent model. In this model, \dot{U}_{ji} is the phase- j i th winding voltage, \dot{I}_{ji} is the phase- j i th winding current, \dot{U}_{sj} is phase- j grid voltage, \dot{I}_{sj} is phase- j grid current, Z_{Kmn} is the short-circuit impedance between m and n winding of the transformer, $Z_{Kk,mn}$ is the equivalent impedance of k winding among the k , m , and n winding of the transformer, \dot{I}_{Lj2h} and \dot{I}_{Lj3h} are the load harmonic current at the MV and LV side, respectively, when all variables are converted to the primary side, $Z_{Kk,mn} = 0.5(Z_{Kkm} + Z_{Kkn} - Z_{Kmn})$, $j = a, b, c, i, k, m, n = 1, 2, 3, 4, k \neq m \neq n$, the subscript h is the h th harmonic.

According to the equivalent decoupling model of the single-phase FW-IFT, the current relational equations can be obtained as follows:

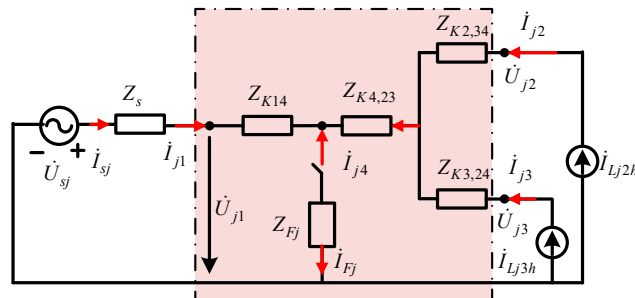
$$\begin{cases} \dot{I}_{j1} = \dot{I}_{sj}; \dot{I}_{j2} = \dot{I}_{Lj2} \\ \dot{I}_{j3} = \dot{I}_{La3}; \dot{I}_{j4} = -\dot{I}_{Fj} \end{cases} \quad (1)$$

Also, the equations concerning both the grid and filtering winding voltage can be obtained as follows:

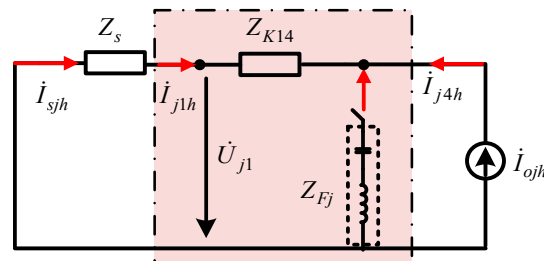
$$\begin{cases} \dot{U}_{j1} = \dot{U}_{sj} - Z_s \dot{I}_{j1} \\ \dot{U}_{j4} = \dot{U}_{Fj} \\ \dot{U}_{Fj} = Z_{Fj} \dot{I}_{Fj} \end{cases} \quad (2)$$



(a)



(b)



(c)

Figure 4. Structure and decoupling circuit. (a) Construction of the FW-IFT, (b) equivalent decoupling circuit model, and (c) simplified resistive equivalent model.

According to the transformer magnetic potential balance principle and ignoring exciting currents, the harmonic magnetic potential balance equation can be obtained as follows:

$$\dot{I}_{j1} + \dot{I}_{j2} + \dot{I}_{j3} + \dot{I}_{j4} = 0 \quad (3)$$

Finally, on the basis of the multi-winding transformer theory, the voltage equations of the FW-IFT can be obtained as follows:

$$\begin{cases} \dot{U}_{j1} - \dot{U}_{j4} = Z_{K14}\dot{I}_{j1} \\ \dot{U}_{j2} - \dot{U}_{j4} = Z_{K24}\dot{I}_{j2} + Z_{K4,23}\dot{I}_{j3} \\ \dot{U}_{j3} - \dot{U}_{j4} = Z_{K4,23}\dot{I}_{j2} + Z_{K34}\dot{I}_{j3} \end{cases} \quad (4)$$

The nonlinear loads at the MV and LV side are equivalent to the harmonic current resources \dot{I}_{Lj2h} , \dot{I}_{Lj3h} , respectively, and considering the possible harmonic voltage from the utility grid, there is also the equivalent harmonic voltage source \dot{U}_{sjh} and system impedance Z_{sh} at the grid side. When the load harmonic currents occur in the MV and LV side, the designed passive filters are connected to the filtering winding of the FW-IFT for implementing inductive filtering. At this time, the h th-order harmonic voltage transfer equations can be obtained as follows:

$$\begin{cases} \dot{U}_{j1h} = (Z_{K14h} + Z_{Fjh})\dot{I}_{sjh} + Z_{Fjh}\dot{I}_{Lj2h} + Z_{Fjh}\dot{I}_{Lj3h} \\ \dot{U}_{j2h} = Z_{Fjh}\dot{I}_{sjh} + (Z_{K24} + Z_{Fjh})\dot{I}_{Lj2h} + Z_{K4,23}\dot{I}_{Lj3h} \\ \dot{U}_{j3h} = Z_{Fjh}\dot{I}_{sjh} + Z_{K4,23}\dot{I}_{Lj2h} + (Z_{K34} + Z_{Fjh})\dot{I}_{Lj3h} \end{cases} \quad (5)$$

Equations (1–5) construct the basic mathematical model of the FW-IFT and the passive filtering branches. This model expresses the constraints among the harmonic voltage, the harmonic current, and the harmonic impedance. Such a mathematical model is useful for operation characteristic research on the inductive filtering technique in HV distribution networks, which contain the FW-IFT and the PFs.

3.2. Harmonic Current Equation

According to the established mathematical model, the equation that expresses the influence of the h th-order harmonic current resources \dot{I}_{Lj2h} , \dot{I}_{Lj3h} at the MV and LV side and the harmonic voltage resource \dot{U}_{sjh} on the h th-order harmonic current \dot{I}_{sjh} in the primary winding can further be obtained by substituting (1), (2) and (3) into (5).

$$\dot{I}_{sjh} = \frac{\dot{U}_{sjh} - Z_{Fjh}\dot{I}_{ojh}}{Z_{sh} + Z_{K14h} + Z_{Fjh}} \quad (6)$$

where the equivalent load harmonic current \dot{I}_{ojh} is set as $\dot{I}_{ojh} = \dot{I}_{Lj2h} + \dot{I}_{Lj3h}$.

Moreover, the equation on the h th-order harmonic current \dot{I}_{Fjh} in the filtering winding can be obtained as follows:

$$\dot{I}_{Fjh} = \frac{\dot{U}_{sjh} + (Z_{sh} + Z_{K14h})\dot{I}_{ojh}}{Z_{sh} + Z_{K14h} + Z_{Fjh}} \quad (7)$$

Equations (6) and (7) reveal the influence of the equivalent impedances of the FW-IFT and the passive filtering branches on the inductive filtering performance.

3.3. Inductive Filtering System Compensation

The inductive filtering system consists of passive filters in series with the filtering winding as shown by a single-phase equivalent decoupling circuit in Figure 4c. Harmonic currents will be induced by these passive filters to offset those of the load side, while the load reactive currents are damped by the IF system. From Equation (6), when the background harmonic voltage $\dot{U}_{sjh} = 0$, the ratio $\dot{I}_{sjh}/\dot{I}_{ojh}$ between the grid harmonic current and the nonlinear load is presented as:

$$\left| \frac{\dot{I}_{sjh}}{\dot{I}_{0jh}} \right|_{\dot{U}_{sjh}=0} = \frac{Z_{Fjh}}{Z_{sh} + Z_{K14h} + Z_{Fjh}} \quad (8)$$

Meanwhile, the ratio $\dot{I}_{sjh}/\dot{I}_{0jh}$ between the grid harmonic current and the nonlinear load is presented as:

$$\left| \frac{\dot{I}_{Fjh}}{\dot{I}_{0jh}} \right|_{\dot{U}_{sjh}=0} = \frac{(Z_{sh} + Z_{K14h})}{Z_{sh} + Z_{K14h} + Z_{Fjh}} \quad (9)$$

The excellent filtering characteristic depends on the impedance value ($Z_{Fjh} \ll Z_{sh} + Z_{K14h}$). The $Z_s + Z_{K14}$ value is always kept higher than the impedance Z_{Fjh} value to improve the filtering characteristic and prevent the harmonic resonance problems between Z_{Fjh} and Z_{K14} . A passive filter impedance is used to compensate for the specific harmonics of interest. Four sets of passive LC (Inductance and capacitance)-filters are tuned to 250 Hz, 350 Hz, 550 Hz, and 650 Hz frequencies to suppress the harmonics at the tuning frequencies. It is worth to note that the nonlinear load produces harmonics at the 5th, 7th, 11th, and 13th harmonic frequencies, so the harmonics will cause a series of problems. Therefore, the filtering branch will induct 5th, 7th, 11th, and 13th dominant harmonics in between the filtering winding and passive LC-filter to offset them, and it advances to stop the flow of harmonic current in the grid winding. The result verifies that the filtering characteristics of the proposed IF method is satisfactory at the 5th (250 Hz), 7th (350 Hz), 11th (550 Hz), and 13th (650 Hz) harmonic frequencies. Figure 5 shows a bode plot of the filtering characteristics of the proposed IF method. The harmonics in Equation (8) in dB and inter-harmonic frequency in Hz are proof of the frequency response of the passive LC-filter. When PF is connected, harmonic damping increases and no amplification phenomena occurs. In addition, all the harmonic content components are considerably reduced as shown in Figure 5. This proves that the proposed IF method is capable of improving the filtering performance, eliminating harmonic amplification phenomena, and compensating for the current harmonic contents produced from the nonlinear load.

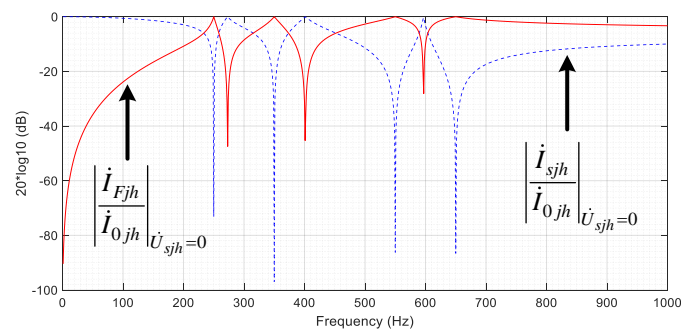


Figure 5. Filtering characteristics of the IF system.

The equivalent impedances of inductive filtering winding for a FW-IFT ($Z_{K4,12}, Z_{K4,13}$) should be designed to be approximately equal to 0; that is to say, $Z_{K4,12} = 0, Z_{K4,13} = 0$, which can satisfy the inductive filtering condition [21]. From Equation (6), it can be seen that the content of the harmonic currents in the primary windings is closely related to the grid-side system impedance Z_{sh} , the short-circuit impedance Z_{K14} , the fully tuned inductive filters' impedance Z_{Fjh} and the grid-side voltage \dot{U}_{sjh} . Ignoring the background harmonic voltage \dot{U}_{sjh} and system impedance Z_{sh} , as long as to ensure that $Z_{Fjh} \approx 0$ of the fully tuned inductive filters at the 5th, 7th, 11th, and 13th harmonic frequencies, then it is ensured that the combined harmonic impedance Z_{Fjh} is much smaller than the short-circuit impedance Z_{K14} , which means that \dot{I}_{sjh} in Equation (6) is close to 0, and there is no or few h th-order harmonic currents generated by the nonlinear loads in the primary winding of the FW-IFT.

$$\dot{I}_{sjh} = 0 \quad (10)$$

In addition, in the ideal condition, i.e., $\dot{U}_{sjh} = 0$, according to Equation (7), the following equation can be further obtained:

$$\dot{I}_{Fjh} = \dot{I}_{ojh} \quad (11)$$

From this, it can be clearly seen that Equation (10), obtained from the equivalent circuit model, verifies the correctness of the established mathematical model. From the above equation, when the harmonic current flows into the load winding of the FW-IFT from the harmonic resource, the filtering winding inducts the corresponding harmonic current to counteract it, and thus, there is no or few inducted harmonic currents at the grid side, as long as the associated harmonic impedances $Z_{K4,12} \approx 0$, $Z_{K4,13} \approx 0$, $Z_{Fah} \approx 0$ can be ensured.

4. Simulation and Experimental Study

4.1. Experimental Model Description

Figure 6 shows the electrical connection of the three-phase experimental system which consists of an ac source, a FW-IFT, three-phase diode rectifier load (as a nonlinear characteristic load), and passive LC filters. This system is designed as a similar model of the HV distribution station shown in Figure 1 (unit No.2). In this experiment, wye-connected primary winding linked with a 380 V ac source, delta-connected filtering winding linked with 220 V passive filters, wye-connected secondary winding linked with 100 V three-phase diode rectifier load, and delta-connected tertiary winding linked with 100 V three-phase diode rectifier load are described in detail.

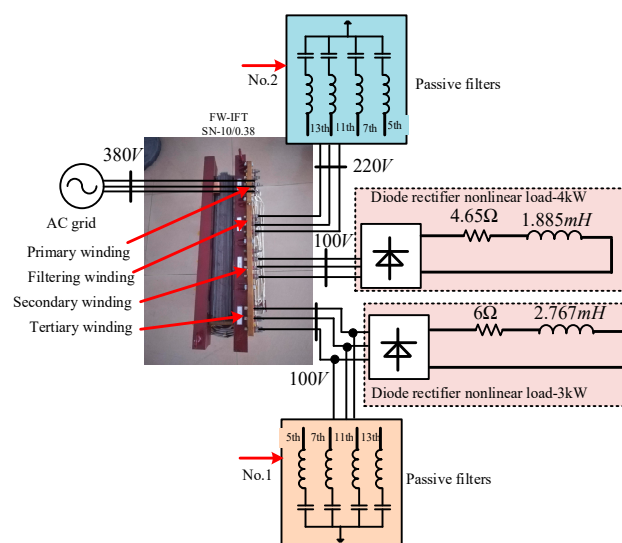


Figure 6. Electrical connection of the experimental system.

Figure 7 shows many components of the experiment, including the prototype of the manufactured FW-IFT, the three-phase diode, ac inductance, the resistance box, and passive filters. Passive filters installed in filtering winding of 220 V is the IF method, while passive filters installed in tertiary winding of 100 V is the IF method. Table 1 summarizes the nameplate parameters of the FW-IFT. Table 2 gives the parameters of four sets of passive filters by comparing the PF method with the IF method. The capacity of each designed passive filter based on both the PF method with the IF method is rated at 200 Var and 50 Var, respectively.



Figure 7. Components of the experimental system.

Table 1. Nameplate parameters of a FW-IFT. HV: high voltage; MV: medium voltage; LV: low voltage; rms: Root Mean Square.

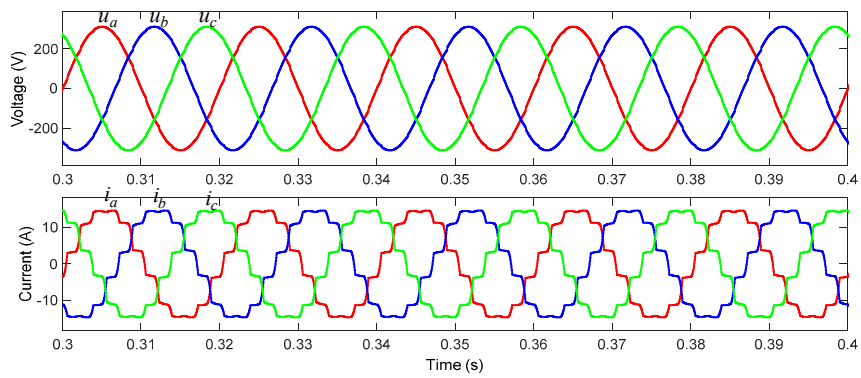
Data	HV-Side	MV-Side	LV-Side	Filtering-Side
Nominal capacity	10 kVA	10 kVA	10 kVA	10 kVA
Nominal line-to-line rms voltage	380 V	100 V	100 V	220 V
Nominal current	15.19 A	57.73 A	57.73 A	26.24 A
Connection	YN	yn0	d11	d11
Short-circuit impedance	$Z_{K12}\% = 5.2$; $Z_{K13}\% = 5.78$; $Z_{K14}\% = 2.83$; $Z_{K23}\% = 2.33$; $Z_{K24}\% = 2.27$; $Z_{K34}\% = 2.75$;			

Table 2. Parameters of filters. PF: passive filtering; IF: inductive filtering; L: inductance; C: capacitance.

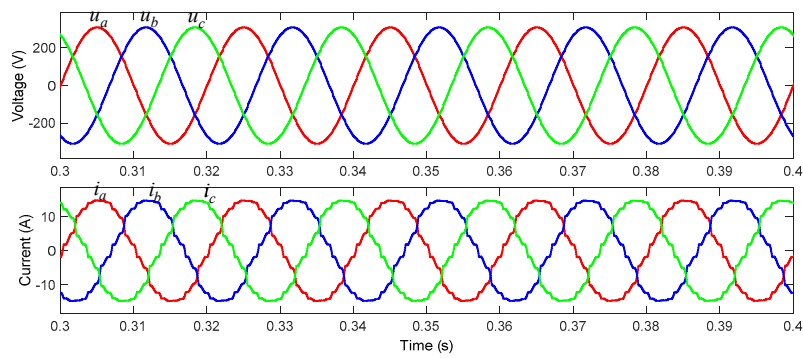
Filtering Method	Parameters	5th	7th	11th	13th
PF	L (mH)	26.562	13.263	5.305	3.789
	C (μ F)	15.279	15.591	15.784	15.821
IF	L (mH)	32.096	16.048	6.419	4.5852
	C (μ F)	12.627	12.885	13.045	13.075

4.2. Simulation Analysis

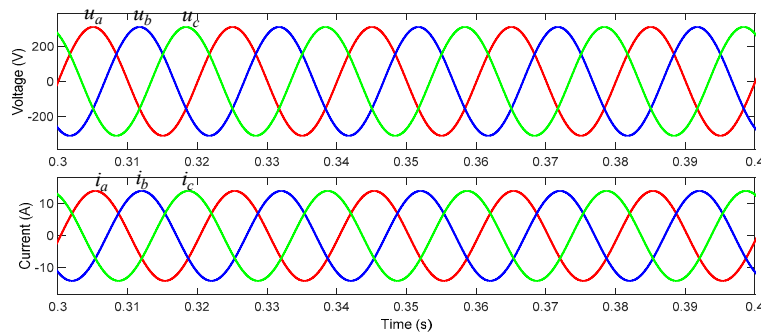
A MATLAB/Simulink based experimental model (seen in Figure 6) is investigated for the IF method with the FW-IFT. The model incorporates the FW-IFT with associated two kinds of diode rectifier circuitry and filtering branches. Figure 8 shows the three-phase voltage and current simulation waveforms, respectively, for without filters, with the PF method, and with the IF method. Filtering performance is compared with the PF method, whose simulation data of grid currents spectra are shown in Figure 9. From Figure 8, grid currents are a non-sinusoidal waveform comprising of lots of 5th, 7th, 11th, and 13th dominant harmonics without filters, which will still exist in the grid side even if the PF method is adopted. However, there are few low-order harmonic currents at the public grid when the IF method is used. From Figure 9, the fundamental rms current amplitude values are 15.01 A, 15.05 A, and 17.87 A, and the current total harmonic distortion (THDi) are 10.51%, 5.62%, and 2.03%, respectively, on the basis of three types of filtering schemes, such as without filters, with PF and with IF. Hence, the simulation results show that the IF method obviously improves the power quality of the grid side.



(a)



(b)



(c)

Figure 8. Grid voltages and currents simulation waveforms. (a) Without filter, (b) the PF method, (c) the IF method.

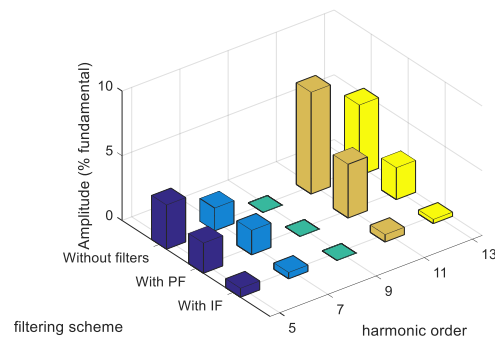


Figure 9. Grid current spectra.

4.3. Experimental Results

Figure 10 shows the three-phase voltage and current measured waveforms at the 380 V bus. Figure 11 shows the phase-A current spectra at the 380 V bus, where the fundamental rms current amplitude values are 14.06 A, 14.75 A, and 16.97 A, and THDi are 10.76%, 5.67%, and 1.63%, respectively, from the three types of filtering scheme (without filters, with PF and with IF).

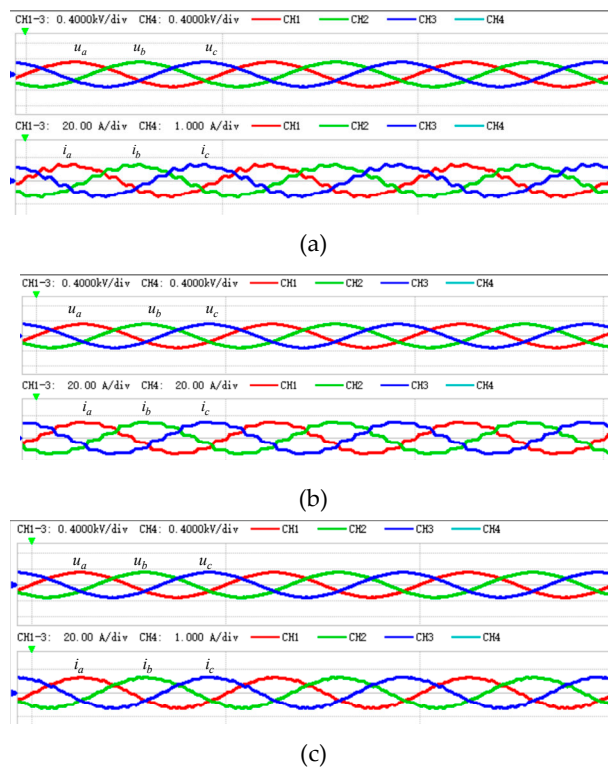


Figure 10. Voltage and current measured waveform at the 380 V bus. (a) Without filter, (b) the PF method, (c) the IF method.

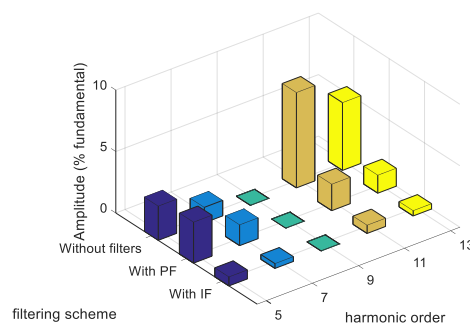


Figure 11. Current spectra at the 380 V bus.

By comparative analysis, it can also be seen that the IF method can greatly reduce the harmonic content in the 380 V bus and the current total harmonic distortion, which can be seen from the fast Fourier transform (FFT) results shown in Figure 11, which drops considerably from 10.76% to 1.63%. Moreover, harmonic currents of the utility grid already meet IEEE Standard 519. Thus, the IF method can not only guarantee the filtering performance on the public grid but can also effectively enhance the power quality for the distribution network supplying nonlinear loads.

5. Conclusions

In this paper, an IF method using a FW-IFT and passive filters for a HV distribution station supplying nonlinear loads has been proposed as a substitute to overcome the shortcomings of the conventional passive filtering method, and this method can comprehensively enhance power quality of the public grid. The single-phase equivalent circuit model and the basic mathematical model of the FW-IFT are established to express such an IF method, and the filtering performance has been analyzed. It was proven that the proposed IF scheme is able to compensate current harmonics simultaneously. The combination of passive filters with a FW-IFT allows for better filtering performance of the nonlinear loads at the MV and/or LV end. An IF method applied in a new HV distribution network has been confirmed to be effective with theoretical, simulation and experimental investigations.

The addition of the filtering winding to the three-winding transformer may bring slight increases, in economical cost, weight, and size, to the FW-IFT. However, the increase may be ignorable from a practical point of view. The proposed system construction is more suitable for a HV distribution network than the PF scheme.

In this paper, the major harmonic suppression of the HV distribution network is investigated in detail. The related research on the steady and transient state characteristics and protection of the FW-IFT will be reported in future.

Author Contributions: All the authors made contributions to the concept and design of the article; Z.H. is the main author of this work. L.L. provided good advice and technical guidance for the manuscript; Y.C., Z.D., P.F. and G.Z. reviewed and polished the manuscript.

Funding: This work was supported by the Hunan province key research and development project under Grant 2017GK2240 and state grid Hunan electric power company under Grant 1618SE-FW.

Conflicts of Interest: The authors declare no conflict of interest.

References

1. Gazafurdi, S.M.M.; Langerudy, A.T.; Fuchs, E.F.; Al-Haddad, K. Power quality issues in railway electrification: A comprehensive perspective. *IEEE Trans. Ind. Electron.* **2015**, *62*, 3081–3090. [[CrossRef](#)]
2. Bubshait, A.S.; Mortezaei, A.; Simoes, M.G.; Busarello, T.D.S. Power Quality Enhancement for a Grid Connected Wind Turbine Energy System. *IEEE Trans. Ind. Appl.* **2017**, *53*, 2495–2505. [[CrossRef](#)]
3. Tareen, W.U.K.; Mekhief, S. Three-Phase Transformerless Shunt Active Power Filter With Reduced Switch Count for Harmonic Compensation in Grid-Connected Applications. *IEEE Trans. Power Electron.* **2018**, *33*, 4868–4881. [[CrossRef](#)]
4. Sheelvant, V.; Kalpana, R.; Singh, B.; Saravana, P.P. Improvement in Harmonic Reduction of a Zigzag Autoconnected Transformer Based 12-Pulse Diode Bridge Rectifier by Current Injection at DC Side. *IEEE Trans. Ind. Appl.* **2017**, *53*, 5634–5644. [[CrossRef](#)]
5. Susovan, M.; Dipten, M.; Ambarnath, B.; Biswas, S.K.; Deb, N.K. A New Harmonic Reduced Three-Phase Thyristor-Controlled Reactor for Static VAR Compensators. *IEEE Trans. Ind. Electron.* **2017**, *64*, 6898–6907.
6. Solanki, J.; Fröhleke, N.; Böcker, J. Implementation of Hybrid Filter for 12-Pulse Thyristor Rectifier Supplying High-Current Variable-Voltage DC Load. *IEEE Trans. Ind. Electron.* **2015**, *62*, 4691–4701. [[CrossRef](#)]
7. Moran, L.; Albistur, C.A.; Burgos, R. Multimega VAR Passive Filters for Mining Applications: Practical Limitations and Technical Considerations. *Trans. Ind. Appl.* **2016**, *52*, 5310–5317. [[CrossRef](#)]
8. Zobaa, A.F.; Aleem, S.H.E.A. A New Approach for Harmonic Distortion Minimization in Power Systems Supplying Nonlinear Loads. *IEEE Trans. Ind. Informat.* **2014**, *10*, 1401–1412. [[CrossRef](#)]
9. Abu-Jalala, A.-H.M.; Cox, T.; Gerada, C.; Rashed, M.; Hamiti, T.; Brown, N. Power Quality Improvement of Synchronous Generators Using an Active Power Filter. *IEEE Trans. Ind. Appl.* **2018**, *54*, 4080–4090. [[CrossRef](#)]
10. Meng, F.; Yang, W.; Yang, S.; Gao, L. Active Harmonic Reduction for 12-Pulse Diode Bridge Rectifier at DC Side with Two-Stage Auxiliary Circuit. *IEEE Trans. Ind. Informat.* **2015**, *11*, 64–73. [[CrossRef](#)]
11. Aleem, S.H.E.A.; Zobaa, A.F.; Aziz, M.M.A. Optimal C-Type Passive Filter Based on Minimization of the Voltage Harmonic Distortion for Nonlinear Loads. *IEEE Trans. Ind. Electron.* **2012**, *59*, 281–288. [[CrossRef](#)]

12. Akagi, H.; Iozaki, K. A Hybrid Active Filter for a Three-Phase 12-Pulse Diode Rectifier Used as the Front End of a Medium-Voltage Motor Drive. *IEEE Trans. Power Electron.* **2012**, *27*, 69–77. [[CrossRef](#)]
13. Chang, G.W.; Wang, H.-L.; Chu, S.-Y. A Probabilistic Approach for Optimal Passive Harmonic Filter Planning. *IEEE Trans. Power Del.* **2007**, *22*, 1790–1798. [[CrossRef](#)]
14. Das, J.C. Passive Filters—Potentialities and Limitations. *IEEE Trans. Ind. Appl.* **2004**, *40*, 232–241. [[CrossRef](#)]
15. Mahanty, R. Large value AC capacitor for harmonic filtering and reactive power compensation. *IET Gener. Transm. Distrib.* **2008**, *2*, 876–891. [[CrossRef](#)]
16. Hamadi, A.; Rahmani, S.; Al-Haddad, K. A Hybrid Passive Filter Configuration for VAR Control and Harmonic Compensation. *IEEE Trans. Ind. Electron.* **2010**, *57*, 2419–2434. [[CrossRef](#)]
17. Salvador, P.; Salmerón, L.P. Reference Voltage Optimization of a Hybrid Filter for Nonlinear Load Compensation. *IEEE Trans. Ind. Electron.* **2014**, *61*, 2648–2654.
18. Wang, L.; Lam, C.-S.; Wong, M.-C. Hybrid Structure of Static Var Compensator and Hybrid Active Power Filter (SVC//HAPF) for Medium-Voltage Heavy Loads Compensation. *IEEE Trans. Ind. Electron.* **2018**, *65*, 4432–4442. [[CrossRef](#)]
19. Lee, T.-L.; Wang, Y.-C.; Li, J.-C.; Guerrero, J.M. Hybrid Active Filter With Variable Conductance for Harmonic Resonance Suppression in Industrial Power Systems. *IEEE Trans. Ind. Electron.* **2015**, *62*, 746–756. [[CrossRef](#)]
20. Li, Y.; Liu, Q.; Hu, S.; Liu, F.; Cao, Y.; Luo, L.; Rehtanz, C. A virtual impedance comprehensive control strategy for the controllably inductive power filtering system. *IEEE Trans. Power Electron.* **2017**, *32*, 920–926. [[CrossRef](#)]
21. Li, Y.; Yao, F.; Cao, Y.; Liu, W.; Liu, F.; Hu, S.; Luo, L.; Zhang, Z.; Chen, Y.; Zhou, G.; et al. An Inductively Filtered Multiwinding Rectifier Transformer and Its Application in Industrial DC Power Supply System. *IEEE Trans. Ind. Electron.* **2016**, *63*, 3987–3997. [[CrossRef](#)]
22. Jazebi, S.; León, F.D. Experimentally validated reversible single-phase multiwinding transformer model for the accurate calculation of low-frequency transients. *IEEE Trans. Power Del.* **2015**, *30*, 193–201. [[CrossRef](#)]



© 2019 by the authors. Licensee MDPI, Basel, Switzerland. This article is an open access article distributed under the terms and conditions of the Creative Commons Attribution (CC BY) license (<http://creativecommons.org/licenses/by/4.0/>).